

# We are IntechOpen, the world's leading publisher of Open Access books Built by scientists, for scientists

6,900

Open access books available

185,000

International authors and editors

200M

Downloads

Our authors are among the

154

Countries delivered to

TOP 1%

most cited scientists

12.2%

Contributors from top 500 universities



WEB OF SCIENCE™

Selection of our books indexed in the Book Citation Index  
in Web of Science™ Core Collection (BKCI)

Interested in publishing with us?  
Contact [book.department@intechopen.com](mailto:book.department@intechopen.com)

Numbers displayed above are based on latest data collected.  
For more information visit [www.intechopen.com](http://www.intechopen.com)



---

# Quantum Walks

---

Takuya Machida

Additional information is available at the end of the chapter

<http://dx.doi.org/10.5772/62481>

---

## Abstract

Quantum walks are quantum counterparts of random walks. While probability distributions of random walks diffusively spread out as the walkers are updating, quantum walks have ballistic behavior. Some of the ballistic behaviors have been revealed in long-time limit theorems and their probability distributions are all far away from the Gaussian distributions, which are known as limit distributions of random walks. In this chapter, we are going to be seeing limit distributions for a standard quantum walk on the line and two kinds of time-dependent quantum walk on the line.

**Keywords:** Quantum walk, limit theorem, Fourier analysis, time-dependent walk, line

---

## 1. Introduction

Quantum walks (QWs) are mathematical models on graphs whose systems repeatedly update according to time-evolution rules. They have been in an emerging field which describes the quantum world. Experts in mathematics, physics, and information theory have been interested in them and to study QWs, and a lot of fascinating properties of QWs have been discovered. Historically, QWs were independently introduced in science from several view points; mathematics in 1988 [1], physics in 1993 [2], and computer science in 1996 [3]. After a while, they began to get attention around 2000. Since QWs can be considered as quantum counterparts of random walks in mathematics, they are also called quantum random walks. The dynamics of QWs are similar to those of random walks in mathematical terms. But, whereas a random walker moves on a graph at random, a quantum walker spreads out as a wave on a graph. Although random walks are stochastic processes, QWs are different. They are unitary processes because the systems of quantum walkers get updated with unitary operators. In quantum physics, the update rules of QWs are interpreted as discretized models of Dirac equations. High

---

dimensional Dirac equations are hard to solve even in numerics due to their complexities, and then we expect QWs to become alternative systems to solve the equations on computer. QWs also play an important role in quantum computers because they are quantum algorithms themselves. Indeed, some quantum algorithms based on QWs show quadratic speed-up, compared to the corresponding classical algorithms [4]. Such algorithms imply that quantum computers could give rise to excellent performance.

In this chapter, we are going to be seeing mathematical aspects of the QWs, which will be described as limit theorems. We first observe a standard QW on the line in Sec.2 Then we shift our focus to time-dependent QWs on the line in Secs. 3 and 4.

## 2. A quantum walk on the line

We start off with the description of a standard QW on the line. The system of the QW is defined in a tensor space of two Hilbert spaces. One is a Hilbert space  $\mathcal{H}_p$  spanned by an orthogonal normalized basis  $\{|x\rangle : x \in \mathbb{Z}\}$ , the other is a Hilbert space  $\mathcal{H}_c$  spanned by an orthogonal normalized basis  $\{|0\rangle, |1\rangle\}$ . We can consider  $|0\rangle$  and  $|1\rangle$  in the Hilbert space  $\mathcal{H}_c$  as the down-spin and the up-spin states of a quantum particle, respectively. The Hilbert space  $\mathcal{H}_p$  is called a position space and the Hilbert space  $\mathcal{H}_c$  is called a coin space. A QW on the line at time  $t$  ( $=0, 1, 2 \dots$ ) is expressed in the tensor Hilbert space,

$$|\Psi_t\rangle = \sum_{x \in \mathbb{Z}} |x\rangle \otimes |\psi_t(x)\rangle \in \mathcal{H}_p \otimes \mathcal{H}_c. \quad (1)$$

Customarily,  $|\psi_t(x)\rangle \in \mathcal{H}_c$  is called a coin state or an amplitude at position  $x$  at time  $t$ . Given an initial state  $|\Psi_0\rangle$ , the walker is repeatedly updating,

$$|\Psi_{t+1}\rangle = SC|\Psi_t\rangle, \quad (2)$$

with

$$C = \sum_{x \in \mathbb{Z}} |x\rangle \langle x| \otimes U, \quad (3)$$

$$S = \sum_{x \in \mathbb{Z}} |x-1\rangle \langle x| \otimes |0\rangle \langle 0| + |x+1\rangle \langle x| \otimes |1\rangle \langle 1|, \quad (4)$$

where  $U$  is a unitary operator. In this chapter, we employ a form of the operator

$$U = \cos\theta|0\rangle\langle 0| + \sin\theta|0\rangle\langle 1| + \sin\theta|1\rangle\langle 0| - \cos\theta|1\rangle\langle 1| \quad (\theta \in [0, 2\pi)), \quad (5)$$

and an initial state

$$|\Psi_0\rangle = |0\rangle \otimes (\alpha|0\rangle + \beta|1\rangle), \quad (6)$$

assuming the complex numbers  $\alpha$  and  $\beta$  satisfy the condition  $|\alpha|^2 + |\beta|^2 = 1$ . The reason that we assigned unitarity to the operator  $U$  and assumed the constraint  $|\alpha|^2 + |\beta|^2 = 1$  is that we define the probability that the quantum walker is observed at position  $x$  at time  $t$ ,

$$\mathbb{P}(X_t = x) = \langle \Psi_t | \left( |x\rangle\langle x| \otimes \sum_{j=0}^1 |j\rangle\langle j| \right) | \Psi_t \rangle, \quad (7)$$

where the random variable  $X_t$  is regarded as the position of the walker at time  $t$ . Thanks to the assignment and the constraint, the right side of Eq. (7) certainly becomes a probability distribution. **Figure 1** shows the probability distribution  $\mathbb{P}(X_t = x)$  at time 500 when the walker starts updating with  $\alpha = 1/\sqrt{2}$  and  $\beta = i/\sqrt{2}$ . In these pictures, only positive values of the probability are plotted. While random walkers normally show diffusive behavior, it is known that the quantum walker acts ballistic as time goes up. We see for certain the ballistic behavior of the probability distribution  $\mathbb{P}(X_t = x)$  in **Figure 2** when we take  $\alpha = 1/\sqrt{2}$  and  $\beta = i/\sqrt{2}$ . As shown in **Figure 1**, the probability distribution  $\mathbb{P}(X_t = x)$  holds two sharp peaks and where they occur strongly depends on the value of the parameter  $\theta$ . We get more detailed information about that from **Figure 3**.

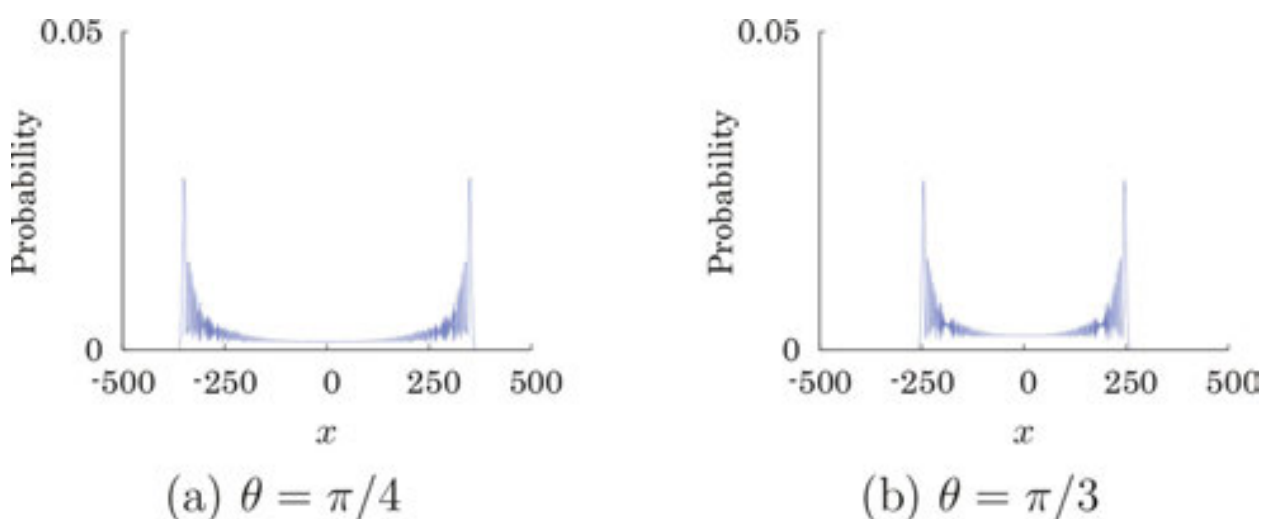


**Figure 1.** Probability distribution at time 500.

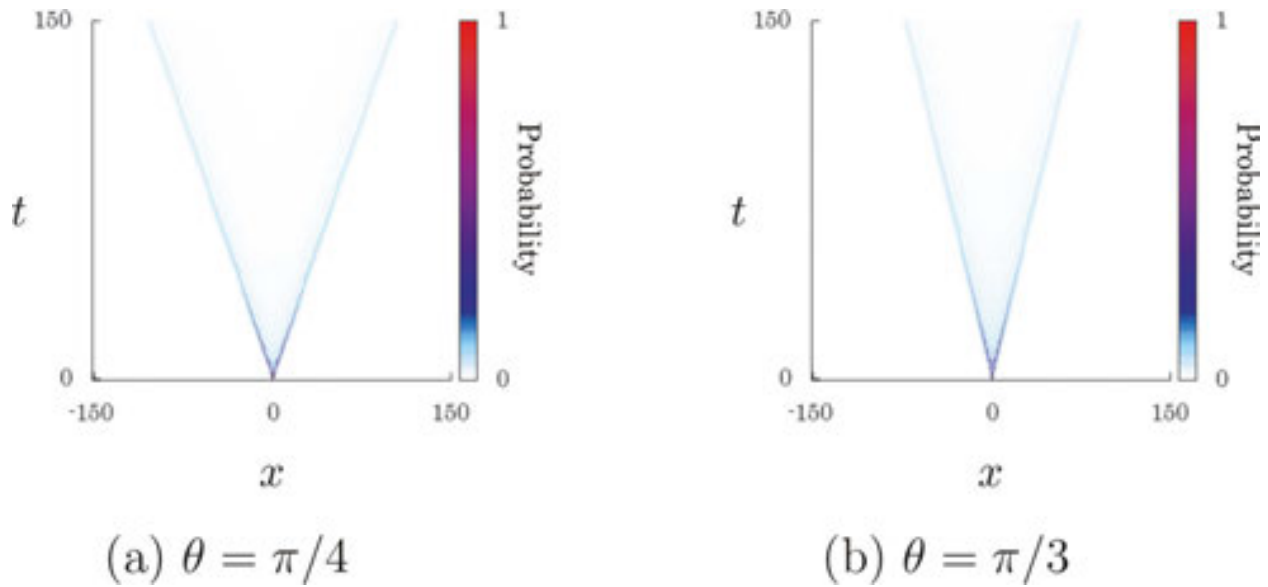


**Figure 2.** Time evolution of the probability distribution  $\mathbb{P}(X_t = x)$ .

The definition of the standard QW on the line has been done. So, what are we curious about? One of the major studies on QWs is to know how their probability distributions behave after they have updated a lot of times. For the probability distribution of the QW defined in this section, one can assert a limit theorem which tells us an approximate behavior of the probability distribution  $\mathbb{P}(X_t = x)$  after time  $t$  goes enough up. First, we see a limit theorem (Theorem 1) when the value of the parameter  $\theta$ , which is embedded in the operator  $U$ , is picked in the interval  $[0, \pi)$ . Then we will extend it for  $\theta \in [0, 2\pi)$  (Theorem 2) which is easily proved by making the most of Theorem 1.

**Theorem 1** Assume that  $\theta \in [0, \pi)$  and  $\theta \neq 0, \pi/2$ . For a real number  $x$ , we have

$$\lim_{t \rightarrow \infty} \mathbb{P} \left( \frac{X_t}{t} \leq x \right) = \int_{-\infty}^x \frac{\sin \theta}{\pi(1-y^2)\sqrt{\cos^2 \theta - y^2}} \times \left[ 1 - \left\{ |\alpha|^2 - |\beta|^2 + \frac{\sin \theta (\alpha \bar{\beta} + \bar{\alpha} \beta)}{\cos \theta} \right\} y \right] I_{(-|\cos \theta|, |\cos \theta|)}(y) dy, \tag{8}$$

where  $I_A(x)$  is an indicator function such that

$$I_A(x) = \begin{cases} 1 & (x \in A) \\ 0 & (\text{otherwise}) \end{cases}. \tag{9}$$

This limit theorem, to be exact which was a theorem for a general unitary operator  $U \in U(2)$ , was proven for the first time by a combinatorial method in 2002 [5]. It was also possible to obtain by Fourier analysis introduced by Grimmett et al. [6]. Here we use the second method to derive the limit theorem. Let  $|\hat{\psi}_t(k)\rangle$  be the Fourier transform of the quantum walker in the form

$$|\hat{\psi}_t(k)\rangle = \sum_{x \in \mathbb{Z}} e^{-ikx} |\psi_t(x)\rangle \quad (k \in [-\pi, \pi]). \quad (10)$$

Oppositely, we can obtain the coin states by inverse Fourier transformation,

$$|\psi_t(x)\rangle = \frac{1}{2\pi} \int_{-\pi}^{\pi} e^{ikx} |\hat{\psi}_t(k)\rangle dk. \quad (11)$$

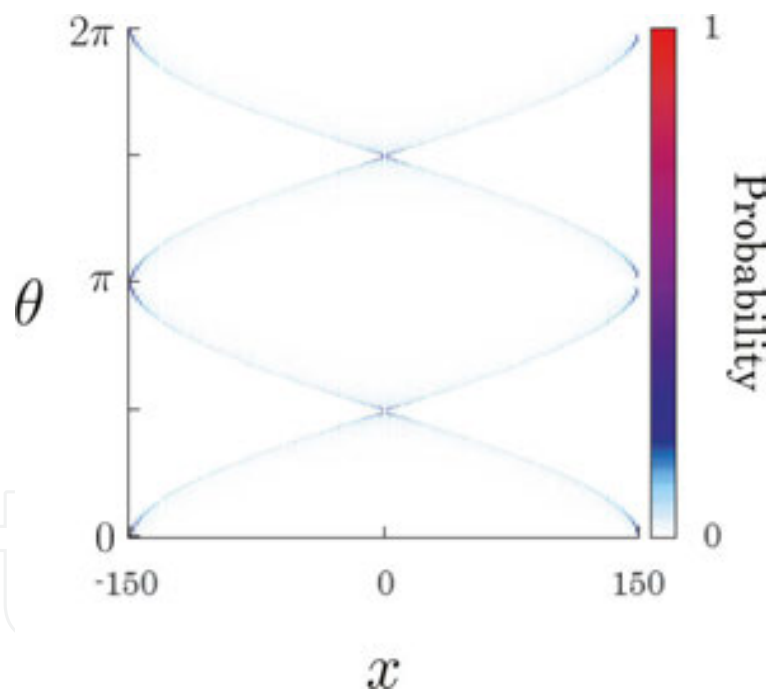


**Figure 3.** This picture shows how the probability distribution at time 150 depends on the value of the parameter  $\theta$ . ( $\alpha = 1/\sqrt{2}$ ,  $\beta = i/\sqrt{2}$ ).

Equation (2) gives the evolution of the Fourier transform,

$$|\hat{\psi}_{t+1}(k)\rangle = R(k)U |\hat{\psi}_t(k)\rangle, \quad (12)$$

with

$$R(k) = e^{ik} |0\rangle \langle 0| + e^{-ik} |1\rangle \langle 1|. \quad (13)$$

The iteration by Eq. (12) connects the system at time  $t$  to the initial state,

$$|\hat{\psi}_t(k)\rangle = (R(k)U)^t |\hat{\psi}_0(k)\rangle. \quad (14)$$

To prove the theorem, we concentrate on a convergence

$$\lim_{t \rightarrow \infty} \mathbb{E}[(X_t / t)^r] = \int_{-\infty}^{\infty} x^r f(x) dx \quad (r = 0, 1, 2, \dots), \quad (15)$$

with

$$f(x) = \frac{\sin \theta}{\pi(1-x^2)\sqrt{\cos^2 \theta - x^2}} \times \left[ 1 - \left\{ |\alpha|^2 - |\beta|^2 + \frac{\sin \theta (\alpha \bar{\beta} + \bar{\alpha} \beta)}{\cos \theta} \right\} x \right] I_{(-|\cos \theta|, |\cos \theta|)}(x). \quad (16)$$

It is known from probability theory that the convergence guarantees Eq. (8). Before we compute the limit, let us depict the  $r$ -th moment  $\mathbb{E}(X_t^r) = \sum_{x=-\infty}^{\infty} x^r \mathbb{P}(X_t = x)$  in Fourier picture. Since the initial state is given by the form of Eq. (6), the Fourier transform at time  $t$  is rewritten in a finite sum

$$|\hat{\psi}_t(k)\rangle = \sum_{x=-\infty}^{\infty} e^{-ikx} |\psi_t(x)\rangle = \sum_{x=-t}^t e^{-ikx} |\psi_t(x)\rangle. \quad (17)$$

Noting that

$$\frac{d^r}{dk^r} |\hat{\psi}_t(k)\rangle = \sum_{x=-t}^t (-ix)^r e^{-ikx} |\psi_t(x)\rangle, \quad (18)$$

we have

$$\begin{aligned} \langle \hat{\psi}_t(k) | i^r \frac{d^r}{dk^r} | \hat{\psi}_t(k) \rangle &= \left( \sum_{x=-t}^t e^{ikx} \langle \psi_t(x) | \right) \left( \sum_{y=-t}^t y^r e^{-iky} | \psi_t(y) \rangle \right) \\ &= \sum_{x=-t}^t \sum_{y=-t}^t x^r e^{ik(x-y)} \langle \psi_t(x) | \psi_t(y) \rangle. \end{aligned} \quad (19)$$

Integrating Eq. (19) over the interval  $[-\pi, \pi)$ , one can generate the  $r$ -th moment of the random variable  $X_t$

$$\begin{aligned} \int_{-\pi}^{\pi} \langle \hat{\psi}_t(k) | i^r \frac{d^r}{dk^r} | \hat{\psi}_t(k) \rangle dk &= \int_{-\pi}^{\pi} \sum_{x=-t}^t \sum_{y=-t}^t y^r e^{ik(x-y)} \langle \psi_t(x) | \psi_t(y) \rangle dk \\ &= 2\pi \sum_{x=-t}^t x^r \langle \psi_t(x) | \psi_t(x) \rangle = 2\pi \sum_{x=-\infty}^{\infty} x^r \langle \psi_t(x) | \psi_t(x) \rangle \\ &= 2\pi \sum_{x=-\infty}^{\infty} x^r \mathbb{P}(X_t = x) = 2\pi \mathbb{E}(X_t^r), \end{aligned} \quad (20)$$

from which the  $r$ -th moment results in a representation in Fourier picture,

$$\mathbb{E}(X_t^r) = \frac{1}{2\pi} \int_{-\pi}^{\pi} \langle \hat{\psi}_t(k) | i^r \frac{d^r}{dk^r} | \hat{\psi}_t(k) \rangle dk. \quad (21)$$

Here, let  $\lambda_j(k)$  ( $j = 1, 2$ ) be the eigenvalues of the matrix  $R(k)U$ , and  $|v_j(k)\rangle$  be the normalized eigenvector associated to the eigenvalue  $\lambda_j(k)$ . Then the initial state of the Fourier transform is decomposed by the normalized eigenvectors,

$$| \hat{\psi}_0(k) \rangle = \langle v_1(k) | \hat{\psi}_0(k) \rangle | v_1(k) \rangle + \langle v_2(k) | \hat{\psi}_0(k) \rangle | v_2(k) \rangle. \quad (22)$$

The Fourier transform at time  $t$  is, therefore, expressed with the eigenvalues and the eigenvectors,

$$| \hat{\psi}_t(k) \rangle = (R(k)U)^t | \hat{\psi}_0(k) \rangle = \sum_{j=1}^2 \lambda_j(k)^t \langle v_j(k) | \hat{\psi}_0(k) \rangle | v_j(k) \rangle, \quad (23)$$

which also gives a description of the derivative

$$\frac{d^r}{dk^r} | \hat{\psi}_t(k) \rangle = (t)_r \cdot \sum_{j=1}^2 \lambda_j(k)^{t-r} \lambda_j'(k)^r \langle v_j(k) | \hat{\psi}_0(k) \rangle | v_j(k) \rangle + O(t^{r-1}), \quad (24)$$

where  $(t)_r = t(t-1)(t-2) \times \dots \times (t-r+1) = \prod_{j=t-r+1}^t j$  and  $\lambda_j'(k) = (d/dk)\lambda_j(k)$ . Recalling the initial state in Eq. (6), we now have the Fourier transform at time 0 in the form

$$|\hat{\psi}_0(k)\rangle = \alpha |0\rangle + \beta |1\rangle. \tag{25}$$

Equations (23) and (24) change the integral picture in Eq. (21),

$$\begin{aligned} \mathbb{E}(X_t^r) &= \frac{1}{2\pi} \int_{-\pi}^{\pi} \langle \hat{\psi}_t(k) | i^r \frac{d^r}{dk^r} | \hat{\psi}_t(k) \rangle dk \\ &= (t)_r \cdot \sum_{j=1}^2 \frac{1}{2\pi} \int_{-\pi}^{\pi} \left( \frac{i\lambda_j'(k)}{\lambda_j(k)} \right)^r |\langle v_j(k) | \hat{\psi}_0(k) \rangle|^2 dk + O(t^{r-1}). \end{aligned} \tag{26}$$

Dividing Eq. (26) by  $t^r$ , we reach a representation

$$\frac{\mathbb{E}(X_t^r)}{t^r} = \frac{(t)_r}{t^r} \cdot \sum_{j=1}^2 \frac{1}{2\pi} \int_{-\pi}^{\pi} \left( \frac{i\lambda_j'(k)}{\lambda_j(k)} \right)^r |\langle v_j(k) | \hat{\psi}_0(k) \rangle|^2 dk + \frac{O(t^{r-1})}{t^r}, \tag{27}$$

and obtain a convergence as  $t \rightarrow \infty$ ,

$$\lim_{t \rightarrow \infty} \mathbb{E} \left[ \left( \frac{X_t}{t} \right)^r \right] = \lim_{t \rightarrow \infty} \frac{\mathbb{E}(X_t^r)}{t^r} = \sum_{j=1}^2 \frac{1}{2\pi} \int_{-\pi}^{\pi} \left( \frac{i\lambda_j'(k)}{\lambda_j(k)} \right)^r |\langle v_j(k) | \hat{\psi}_0(k) \rangle|^2 dk. \tag{28}$$

Now what we need more has made sense. It is the eigensystem of the operator  $R(k)U$ . To make a computation about it, we give a standard basis to the Hilbert space  $\mathcal{H}_\sigma$

$$|0\rangle = \begin{bmatrix} 1 \\ 0 \end{bmatrix}, \quad |1\rangle = \begin{bmatrix} 0 \\ 1 \end{bmatrix}, \tag{29}$$

from which a matrix representation follows,

$$R(k)U = \begin{bmatrix} e^{ik} \cos \theta & e^{ik} \sin \theta \\ e^{-ik} \sin \theta & -e^{-ik} \cos \theta \end{bmatrix}. \tag{30}$$

The matrix contains two different eigenvalues

$$\lambda_j(k) = -(-1)^j \sqrt{1 - c^2 \sin^2 k} + ic \sin k \quad (j = 1, 2), \quad (31)$$

in which  $c$  and  $s$  are short for  $\cos\theta$  and  $\sin\theta$ , respectively. Differentiating Eq. (31) with respect to the variable  $k$ , we get

$$\lambda_j'(k) = -(-1)^j \frac{ic \cos k}{\sqrt{1 - c^2 \sin^2 k}} \left\{ -(-1)^j \sqrt{1 - c^2 \sin^2 k} + ic \sin k \right\}, \quad (32)$$

from which the function  $i\lambda_j'(k)/\lambda_j(k)$  is computed,

$$\frac{i\lambda_j'(k)}{\lambda_j(k)} = (-1)^j \frac{c \cos k}{\sqrt{1 - c^2 \sin^2 k}}. \quad (33)$$

The normalized eigenvector associated to the eigenvalue  $\lambda_j(k)$  has a form

$$|v_j(k)\rangle = \frac{1}{\sqrt{N_j(k)}} \begin{bmatrix} se^{ik} \\ -c \cos k - (-1)^j \sqrt{1 - c^2 \sin^2 k} \end{bmatrix}, \quad (34)$$

with its normalized factor

$$N_j(k) = 2\sqrt{1 - c^2 \sin^2 k} \left\{ \sqrt{1 - c^2 \sin^2 k} + (-1)^j c \cos k \right\}. \quad (35)$$

Back in Eq. (28), we put  $i\lambda_j'(k)/\lambda_j(k) = x(j = 1, 2)$  and then obtain another integral form

$$\begin{aligned}
 \lim_{t \rightarrow \infty} \mathbb{E} \left[ \left( \frac{X_t}{t} \right)^r \right] &= \sum_{j=1}^2 \frac{1}{2\pi} \int_{-\pi}^{\pi} \left( \frac{i\lambda'_j(k)}{\lambda_j(k)} \right)^r \left| \langle v_j(k) | \hat{\psi}_0(k) \rangle \right|^2 dk \\
 &= \int_{-c}^c x^r \frac{|c|s}{\pi c(1-x^2)\sqrt{c^2-x^2}} \left[ 1 - \left\{ |\alpha|^2 - |\beta|^2 + \frac{s(\alpha\bar{\beta} + \bar{\alpha}\beta)}{c} \right\} x \right] dx \\
 &= \int_{-|c|}^{|c|} x^r \frac{s}{\pi(1-x^2)\sqrt{c^2-x^2}} \left[ 1 - \left\{ |\alpha|^2 - |\beta|^2 + \frac{s(\alpha\bar{\beta} + \bar{\alpha}\beta)}{c} \right\} x \right] dx \\
 &= \int_{-\infty}^{\infty} x^r \frac{s}{\pi(1-x^2)\sqrt{c^2-x^2}} \\
 &\quad \times \left[ 1 - \left\{ |\alpha|^2 - |\beta|^2 + \frac{s(\alpha\bar{\beta} + \bar{\alpha}\beta)}{c} \right\} x \right] I_{(-|c|,|c|)}(x) dx.
 \end{aligned} \tag{36}$$

Equation (36) allows us to hold Eq. (8).

Now that we have obtained a limit theorem for the QW whose operator was defined by

$$U = \cos\theta |0\rangle \langle 0| + \sin\theta |0\rangle \langle 1| + \sin\theta |1\rangle \langle 0| - \cos\theta |1\rangle \langle 1| \quad (\theta \in [0, \pi]), \tag{37}$$

Theorem 1 can be extended for the parameter  $\theta \in [0, 2\pi)$ .

**Theorem 2** Assume that  $\theta \in [0, 2\pi)$  and  $\theta \neq 0, \pi/2, \pi, 3\pi/2$ . For a real number  $x$ , we have

$$\begin{aligned}
 \lim_{t \rightarrow \infty} \mathbb{P} \left( \frac{X_t}{t} \leq x \right) &= \int_{-\infty}^x \frac{|\sin\theta|}{\pi(1-y^2)\sqrt{\cos^2\theta - y^2}} \\
 &\quad \times \left[ 1 - \left\{ |\alpha|^2 - |\beta|^2 + \frac{\sin\theta(\alpha\bar{\beta} + \bar{\alpha}\beta)}{\cos\theta} \right\} y \right] I_{(-|\cos\theta|, |\cos\theta|)}(y) dy.
 \end{aligned} \tag{38}$$

Since we already had the limit theorem for the parameter  $\theta \in [0, \pi)$  as Theorem 1, it is enough to prove Theorem 2 for  $\theta \in [\pi, 2\pi)$  ( $\theta \neq \pi, 3\pi/2$ ). Do you think we have to carry out the same calculation for such a parameter again? We do not actually have to do that and can avoid the same math by applying a small skill to the operator  $U$ . Let us slightly change the form of the operator  $U$ , which is described by  $U(\theta)$  below,

$$\begin{aligned}
 U(\theta) &:= U = \cos\theta |0\rangle \langle 0| + \sin\theta |0\rangle \langle 1| + \sin\theta |1\rangle \langle 0| - \cos\theta |1\rangle \langle 1| \\
 &= -\{ \cos(\theta - \pi) |0\rangle \langle 0| + \sin(\theta - \pi) |0\rangle \langle 1| \\
 &\quad + \sin(\theta - \pi) |1\rangle \langle 0| - \cos(\theta - \pi) |1\rangle \langle 1| \} = -U(\theta - \pi).
 \end{aligned} \tag{39}$$

The negative sign in front of the operator  $U(\theta - \pi)$  in Eq. (39) does not affect the probability distribution  $\mathbb{P}(X_t = x)$ , which means the probability distribution given by the operator  $U(\theta)$  is completely same as that given by the operator  $U(\theta - \pi)$ . Moreover, as long as the parameter  $\theta$  picks a value in the interval  $[\pi, 2\pi)$ , the variable  $\theta - \pi$  stays in the interval  $[0, \pi)$ . Since Theorem 1 works on the QW operated by  $U(\theta - \pi)$  ( $\theta \in [\pi, 2\pi)$ ), one can assert a limit theorem for the parameter  $\theta \in [\pi, 2\pi)$ ,

$$\begin{aligned} & \lim_{t \rightarrow \infty} \mathbb{P}\left(\frac{X_t}{t} \leq x\right) \\ &= \int_{-\infty}^x \frac{\sin(\theta - \pi)}{\pi(1 - y^2)\sqrt{\cos^2(\theta - \pi) - y^2}} \left[ 1 - \left\{ |\alpha|^2 - |\beta|^2 \right. \right. \\ & \quad \left. \left. + \frac{\sin(\theta - \pi)(\bar{\alpha}\beta + \bar{\alpha}\beta)}{\cos(\theta - \pi)} \right\} y \right] I_{(-|\cos(\theta - \pi)|, |\cos(\theta - \pi)|)}(y) dy \\ &= \int_{-\infty}^x \frac{-\sin \theta}{\pi(1 - y^2)\sqrt{\cos^2 \theta - y^2}} \\ & \times \left[ 1 - \left\{ |\alpha|^2 - |\beta|^2 + \frac{\sin \theta(\bar{\alpha}\beta + \bar{\alpha}\beta)}{\cos \theta} \right\} y \right] I_{(-|\cos \theta|, |\cos \theta|)}(y) dy \end{aligned} \tag{40}$$

We should remark that Eq. (40) holds under the condition  $\theta - \pi \neq 0, \pi/2$ , that is,  $\theta \neq \pi, 3\pi/2$ . As a consequence of Theorem 1 and Eq. (40), Theorem 2 comes up.

**Figure 4** shows an example of the limit density function.

$$\begin{aligned} & \frac{d}{dx} \lim_{t \rightarrow \infty} \mathbb{P}\left(\frac{X_t}{t} \leq x\right) \\ &= \frac{|\sin \theta|}{\pi(1 - x^2)\sqrt{\cos^2 \theta - x^2}} \\ & \times \left[ 1 - \left\{ |\alpha|^2 - |\beta|^2 + \frac{\sin \theta(\bar{\alpha}\beta + \bar{\alpha}\beta)}{\cos \theta} \right\} x \right] I_{(-|\cos \theta|, |\cos \theta|)}(x) dy. \end{aligned} \tag{41}$$

We see that the limit density function reproduces the features of the probability distribution shown in **Figure 1**.

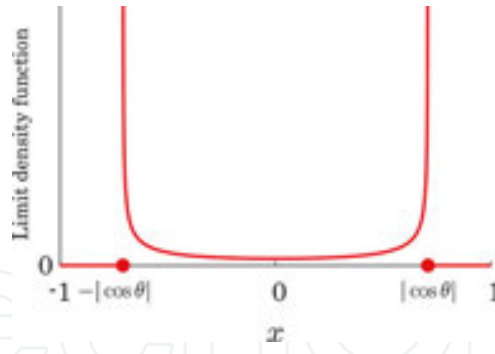


Figure 4. The limit density function ( $\alpha = 1/\sqrt{2}$ ,  $\beta = i/\sqrt{2}$ ).

### 3. Two-period time-dependent QW

In this section, we see a time-dependent QW whose coin-flip operator depends on time. The evolution of the QW is given by two unitary operators,

$$\begin{aligned}
 U_1 &= \cos\theta_1 |0\rangle\langle 0| + \sin\theta_1 |0\rangle\langle 1| + \sin\theta_1 |1\rangle\langle 0| - \cos\theta_1 |1\rangle\langle 1| \\
 &= c_1 |0\rangle\langle 0| + s_1 |0\rangle\langle 1| + s_1 |1\rangle\langle 0| - c_1 |1\rangle\langle 1|,
 \end{aligned}
 \tag{42}$$

$$\begin{aligned}
 U_2 &= \cos\theta_2 |0\rangle\langle 0| + \sin\theta_2 |0\rangle\langle 1| + \sin\theta_2 |1\rangle\langle 0| - \cos\theta_2 |1\rangle\langle 1| \\
 &= c_2 |0\rangle\langle 0| + s_2 |0\rangle\langle 1| + s_2 |1\rangle\langle 0| - c_2 |1\rangle\langle 1|,
 \end{aligned}
 \tag{43}$$

with  $\theta_j \in [0, 2\pi)$  ( $j = 1, 2$ ), and  $\cos\theta_j$  (resp.  $\sin\theta_j$ ) has been briefly written as  $c_j$  (resp.  $s_j$ ). The total system at time  $t$  evolves to the next state at time  $t + 1$  according to the time evolution rule

$$|\Psi_{t+1}\rangle = \begin{cases} SC_1 |\Psi_t\rangle & (t = 0, 2, 4, \dots) \\ SC_2 |\Psi_t\rangle & (t = 1, 3, 5, \dots) \end{cases}
 \tag{44}$$

where

$$C_j = \sum_{x \in \mathbb{Z}} |x\rangle\langle x| \otimes U_j \quad (j = 1, 2).
 \tag{45}$$

It is plain that the operators  $C_1$  and  $C_2$  are alternately casted on the QW, which means that the unitary operator 2-periodically changes in time-line. If the parameters  $\theta_1$  and  $\theta_2$  take the same value, then the QW becomes the standard walk defined in Sec.

Now, we are looking at examples of the probability distribution when the walker starts off with  $|\Psi_0\rangle = |0\rangle \otimes (1/\sqrt{2} |0\rangle + i/\sqrt{2} |1\rangle)$ . **Figure 5** draws the probability distribution at time 500

and two sharp peaks are observed in each picture. In the pictures, only positive values of probability are plotted. As shown in **Figure 6**, the probability distribution is spreading in proportion to time  $t$ . We also see how it depends on the parameters  $\theta_1$  and  $\theta_2$  in **Figure 7**.

The features, which we have seen in **Figures 5 to 7** are caught by a limit theorem.

**Theorem 3** Assume that  $\theta_1, \theta_2 \neq 0, \pi/2, \pi, 3\pi/2$ . For a real number  $x$ , we have

$$\lim_{t \rightarrow \infty} \mathbb{P} \left( \frac{X_t}{t} \leq x \right) = \int_{-\infty}^x \frac{\sqrt{1 - \xi(\theta_1, \theta_2)^2}}{\pi(1 - y^2)\sqrt{\xi(\theta_1, \theta_2)^2 - y^2}} \times \left[ 1 - \left\{ |\alpha|^2 - |\beta|^2 + \frac{\sin \theta_1 (\alpha \bar{\beta} + \bar{\alpha} \beta)}{\cos \theta_1} \right\} y \right] I_{(-\xi(\theta_1, \theta_2), \xi(\theta_1, \theta_2))}(y) dy, \quad (46)$$

with  $\xi(\theta_1, \theta_2) = \min\{|\cos \theta_1|, |\cos \theta_2|\}$ .

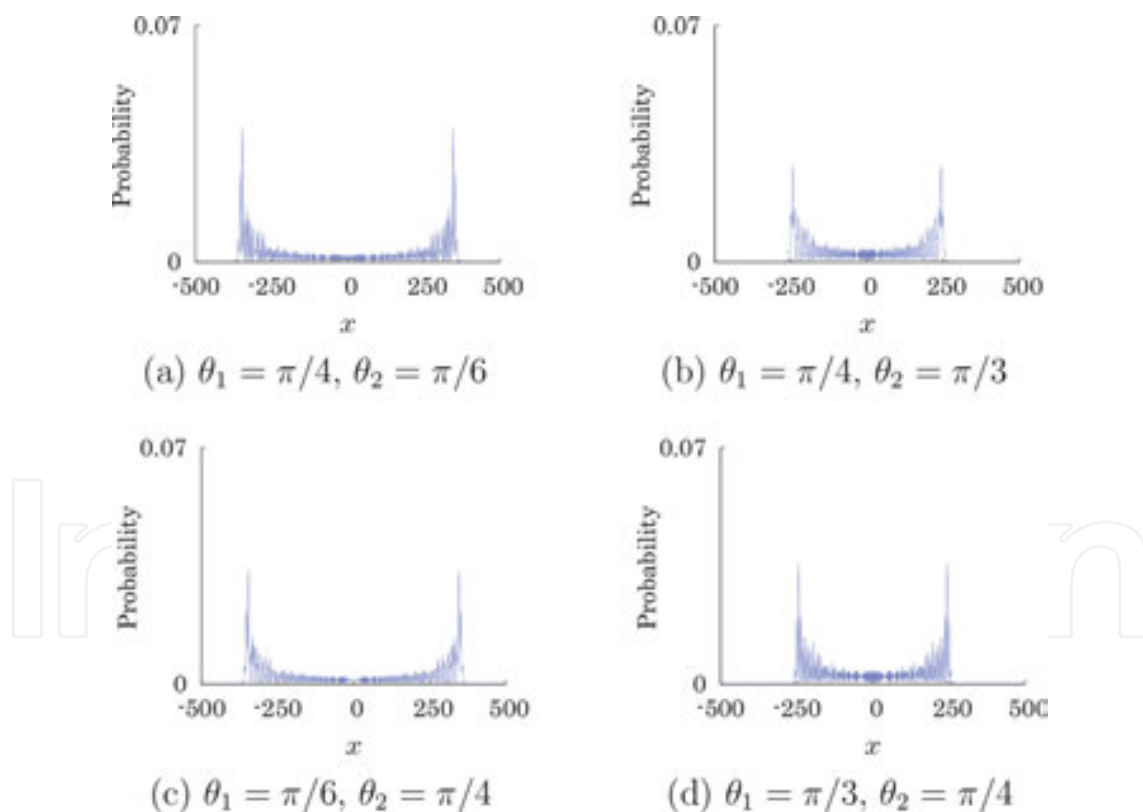


**Figure 5.** Probability distribution at time 500 ( $\alpha = 1/\sqrt{2}, \beta = i/\sqrt{2}$ ).

This limit theorem was proved by Fourier analysis in 2010 [7]. First, we find the time evolution of the Fourier transform  $|\hat{\psi}_t(k)\rangle = \sum_{x \in \mathbb{Z}} e^{-ikx} |\psi_t(x)\rangle$  ( $k \in [-\pi, \pi)$ ),

$$|\hat{\psi}_{i+1}(k)\rangle = \begin{cases} R(k)U_1 |\hat{\psi}_i(k)\rangle & (t = 0, 2, 4, \dots) \\ R(k)U_2 |\hat{\psi}_i(k)\rangle & (t = 1, 3, 5, \dots) \end{cases} \quad (47)$$

which comes from Eq. (44). We should recall  $R(k) = e^{ik}|0\rangle\langle 0| + e^{-ik}|1\rangle\langle 1|$ . From the recurrence, the transform at each time gets a connection to its initial state,

$$|\hat{\psi}_{2t}(k)\rangle = (R(k)U_2 R(k)U_1)^t |\hat{\psi}_0(k)\rangle, \quad (48)$$

$$|\hat{\psi}_{2t+1}(k)\rangle = R(k)U_1 (R(k)U_2 R(k)U_1)^t |\hat{\psi}_0(k)\rangle. \quad (49)$$

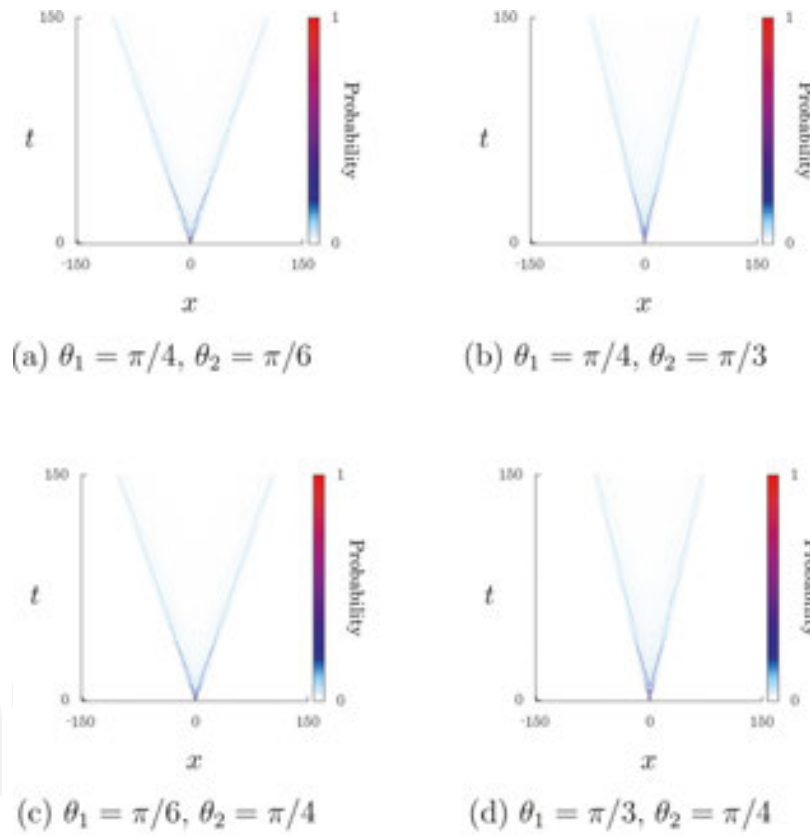


**Figure 6.** Time evolution of the probability distribution ( $\alpha = 1/\sqrt{2}$ ,  $\beta = i/\sqrt{2}$ ).

The eigensystem of the matrix  $R(k)U_2 R(k)U_1$  reforms Eqs. (48) and (49),

$$|\hat{\psi}_{2t}(k)\rangle = \sum_{j=1}^2 \lambda_j(k)^t \langle v_j(k) | \hat{\psi}_0(k) \rangle |v_j(k)\rangle, \quad (50)$$

$$|\hat{\psi}_{2t+1}(k)\rangle = R(k)U_1 \sum_{j=1}^2 \lambda_j(k)^t \langle v_j(k) | \hat{\psi}_0(k) \rangle |v_j(k)\rangle. \quad (51)$$

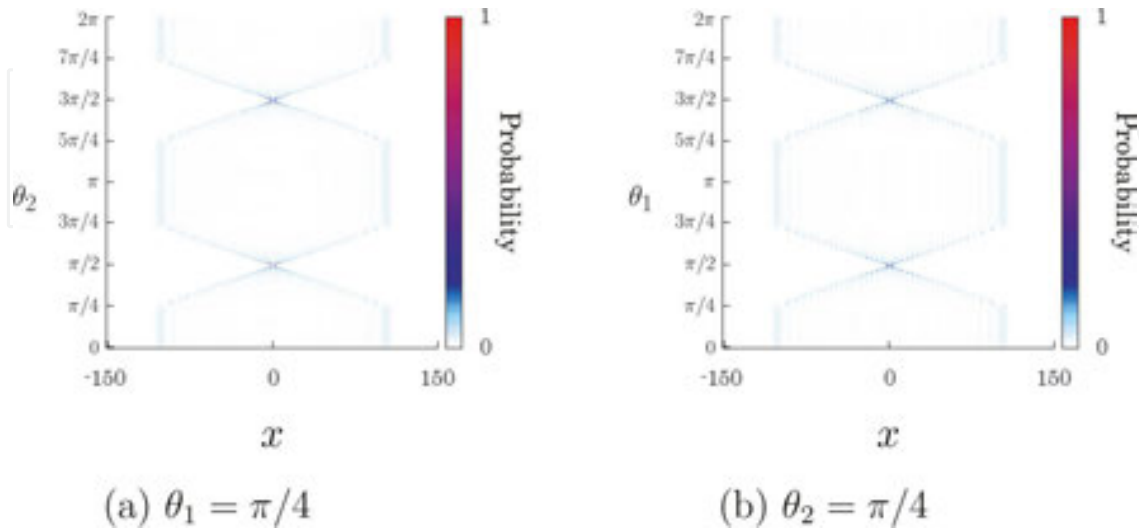


**Figure 7.** These pictures show how the probability distribution at time 150 depends on the value of the parameters  $\theta_1$  and  $\theta_2$  ( $\alpha=1/\sqrt{2}$ ,  $\beta=i/\sqrt{2}$ ).

Arranging the  $r$ -th derivatives ( $r = 0, 1, 2, \dots$ ) of the Fourier transform on the scale of time  $t$ ,

$$\frac{d^r}{dk^r} |\hat{\psi}_{2t}(k)\rangle = (t)_r \cdot \sum_{j=1}^2 \lambda_j(k)^{t-r} \lambda_j(k)^r \langle v_j(k) | \hat{\psi}_0(k) \rangle |v_j(k)\rangle + O(t^{r-1}), \quad (52)$$

$$\begin{aligned} \frac{d^r}{dk^r} |\hat{\psi}_{2t+1}(k)\rangle &= (t)_r \cdot R(k)U_1 \sum_{j=1}^2 \lambda_j(k)^{t-r} \lambda_j(k)^r \langle v_j(k) | \hat{\psi}_0(k) \rangle |v_j(k)\rangle \\ &+ O(t^{r-1}), \end{aligned} \quad (53)$$

we obtain the representations of the  $r$ -th moment of the random variable  $X_{2t}$

$$\mathbb{E}(X_{2t}^r) = (t)_r \cdot \sum_{j=1}^2 \frac{1}{2\pi} \int_{-\pi}^{\pi} \left( \frac{i\lambda_j(k)}{\lambda_j(k)} \right)^r |\langle v_j(k) | \hat{\psi}_0(k) \rangle|^2 dk + O(t^{r-1}), \quad (54)$$

$$\mathbb{E}(X_{2t+1}^r) = (t)_r \cdot \sum_{j=1}^2 \frac{1}{2\pi} \int_{-\pi}^{\pi} \left( \frac{i\lambda_j(k)}{\lambda_j(k)} \right)^r |\langle v_j(k) | \hat{\psi}_0(k) \rangle|^2 dk + O(t^{r-1}). \quad (55)$$

Dividing these equations by time  $2t$  or  $2t + 1$  followed by taking a limit makes the same expression,

$$\lim_{t \rightarrow \infty} \frac{\mathbb{E}(X_{2t}^r)}{(2t)^r} = \sum_{j=1}^2 \frac{1}{2\pi} \int_{-\pi}^{\pi} \left( \frac{i\lambda_j'(k)}{2\lambda_j(k)} \right)^r |\langle v_j(k) | \hat{\psi}_0(k) \rangle|^2 dk, \quad (56)$$

$$\begin{aligned} \lim_{t \rightarrow \infty} \frac{\mathbb{E}(X_{2t+1}^r)}{(2t+1)^r} &= \lim_{t \rightarrow \infty} \frac{\mathbb{E}(X_{2t+1}^r)}{(2t)^r} \cdot \left( \frac{2t}{2t+1} \right)^r \\ &= \sum_{j=1}^2 \frac{1}{2\pi} \int_{-\pi}^{\pi} \left( \frac{i\lambda_j'(k)}{2\lambda_j(k)} \right)^r |\langle v_j(k) | \hat{\psi}_0(k) \rangle|^2 dk, \end{aligned} \quad (57)$$

which are combined as

$$\begin{aligned} \lim_{t \rightarrow \infty} \mathbb{E} \left[ \left( \frac{X_{2t}}{2t} \right)^r \right] &= \lim_{t \rightarrow \infty} \mathbb{E} \left[ \left( \frac{X_{2t+1}}{2t+1} \right)^r \right] \\ &= \sum_{j=1}^2 \frac{1}{2\pi} \int_{-\pi}^{\pi} \left( \frac{i\lambda_j'(k)}{2\lambda_j(k)} \right)^r |\langle v_j(k) | \hat{\psi}_0(k) \rangle|^2 dk. \end{aligned} \quad (58)$$

As a result, we have

$$\lim_{t \rightarrow \infty} \mathbb{E} \left[ \left( \frac{X_t}{t} \right)^r \right] = \sum_{j=1}^2 \frac{1}{2\pi} \int_{-\pi}^{\pi} \left( \frac{i\lambda_j'(k)}{2\lambda_j(k)} \right)^r |\langle v_j(k) | \hat{\psi}_0(k) \rangle|^2 dk. \quad (59)$$

The Hilbert space  $\mathcal{H}_c$  spanned by Eq. (29) gives a matrix representation to the operator  $R(k)U_2R(k)U_1$ ,

$$R(k)U_2R(k)U_1 = \begin{bmatrix} c_1c_2e^{2ik} + s_1s_2 & s_1c_2e^{2ik} - c_1s_2 \\ -s_1c_2e^{-2ik} + c_1s_2 & c_1c_2e^{-2ik} + s_1s_2 \end{bmatrix}, \quad (60)$$

and one can find its eigenvalues

$$\lambda_j(k) = c_1c_2 \cos 2k + s_1s_2 - (-1)^j i \sqrt{1 - (c_1c_2 \cos 2k + s_1s_2)^2} \quad (j = 1, 2). \quad (61)$$

The normalized eigenvector associated to the eigenvalue  $\lambda_j(k)$  takes a form

$$|v_j(k)\rangle = \frac{1}{\sqrt{N_j(k)}} \left[ i \left\{ -c_1 c_2 \sin 2k - (-1)^j \sqrt{1 - (c_1 c_2 \cos 2k + s_1 s_2)^2} \right\} \right], \quad (62)$$

with

$$N_j(k) = 1 - (c_1^2 - s_1^2)(c_2^2 - s_2^2) - 4c_1 c_2 s_1 s_2 \cos 2k + 2c_1^2 c_2^2 \sin^2 2k + (-1)^j 2c_1 c_2 \sin 2k \sqrt{1 - (c_1 c_2 \cos 2k + s_1 s_2)^2}. \quad (63)$$

Here we compute

$$\frac{i\lambda_j'(k)}{2\lambda_j(k)} = (-1)^j \frac{c_1 c_2 \sin 2k}{\sqrt{1 - (c_1 c_2 \cos 2k + s_1 s_2)^2}}, \quad (64)$$

from Eq. (61). Putting  $i\lambda_j'(k)/2\lambda_j(k) = x$  ( $j = 1, 2$ ) gives rise to another expression of Eq. (59),

$$\lim_{t \rightarrow \infty} \mathbb{E} \left[ \left( \frac{X_t}{t} \right)^r \right] = \int_{-\infty}^{\infty} x^r \frac{\sqrt{1 - \xi(\theta_1, \theta_2)^2}}{\pi(1 - x^2) \sqrt{\xi(\theta_1, \theta_2)^2 - x^2}} \times \left[ 1 - \left\{ |\alpha|^2 - |\beta|^2 + \frac{\sin \theta_1 (\alpha \bar{\beta} + \bar{\alpha} \beta)}{\cos \theta_1} \right\} x \right] I_{(-\xi(\theta_1, \theta_2), \xi(\theta_1, \theta_2))}(x) dx. \quad (65)$$

For the same reason as the proof for Theorem 1, this convergence promises Theorem 3. As mentioned earlier, if the parameters  $\theta_1$  and  $\theta_2$  take the same value  $\theta$ , then the 2-period time-dependent QW is the standard walk shown in Sec.2. In that case, Theorem 3 is in agreement with Theorem 2. Indeed, inserting a value, which is supposed to be  $\theta$  now, to both  $\theta_1$  and  $\theta_2$  in Theorem 2 produces the limit probability distribution below,

$$\lim_{t \rightarrow \infty} \mathbb{P} \left( \frac{X_t}{t} \leq x \right) = \int_{-\infty}^x \frac{|\sin \theta|}{\pi(1 - y^2) \sqrt{\cos^2 \theta - y^2}} \times \left[ 1 - \left\{ |\alpha|^2 - |\beta|^2 + \frac{\sin \theta (\alpha \bar{\beta} + \bar{\alpha} \beta)}{\cos \theta} \right\} y \right] I_{(-|\cos \theta|, |\cos \theta|)}(y) dy. \quad (66)$$

Given an initial state with  $\alpha = 1/\sqrt{2}$ ,  $\beta = i/\sqrt{2}$ , **Figure 8** draws the limit density function

$$\frac{d}{dx} \lim_{t \rightarrow \infty} \mathbb{P} \left( \frac{X_t}{t} \leq x \right) = \frac{\sqrt{1 - \xi(\theta_1, \theta_2)^2}}{\pi(1 - x^2) \sqrt{\xi(\theta_1, \theta_2)^2 - x^2}} I_{(-\xi(\theta_1, \theta_2), \xi(\theta_1, \theta_2))}(x). \tag{67}$$

We confirm that the function has two singularities at the points  $\pm \xi(\theta_1, \theta_2)$  which correspond to two sharp peaks in **Figure 5**.

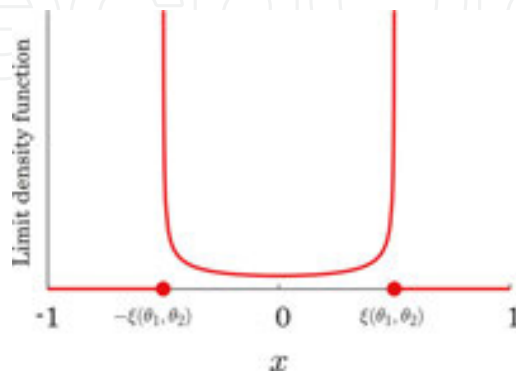


**Figure 8.** Limit density function ( $\alpha = 1/\sqrt{2}$ ,  $\beta = i/\sqrt{2}$ ).

### 4. Three-period time-dependent QW

The standard QW in Sec.2 and the two-period time-dependent QW in Sec.3 have the same type of limit density function. In the final section, we see a three-period time-dependent QW and its limit density function. As a result, a different type of limit density function will be discovered. With a unitary operator  $U \in U(2)$ , the system of three-period time-dependent QW is periodically updating,

$$|\Psi_{t+1}\rangle = \begin{cases} SC|\Psi_t\rangle & (t = 0, 3, 5, \dots) \\ SC|\Psi_t\rangle & (t = 1, 4, 6, \dots), \\ S|\Psi_t\rangle & (t = 2, 5, 7, \dots) \end{cases} \tag{68}$$

where

$$C = \sum_{x \in \mathbb{Z}} |x\rangle \langle x| \otimes U, \tag{69}$$

$$S = \sum_{x \in \mathbb{Z}} |x-1\rangle \langle x| \otimes |0\rangle \langle 0| + |x+1\rangle \langle x| \otimes |1\rangle \langle 1|. \tag{70}$$

The 3-period time-dependent QW was studied by Grünbaum and Machida [8] when the unitary operator  $U$  was of the form

$$\begin{aligned}
 U &= \cos\theta |0\rangle\langle 0| + \sin\theta |0\rangle\langle 1| + \sin\theta |1\rangle\langle 0| - \cos\theta |1\rangle\langle 1| \\
 &= c |0\rangle\langle 0| + s |0\rangle\langle 1| + s |1\rangle\langle 0| - c |1\rangle\langle 1|,
 \end{aligned}
 \tag{71}$$

with  $\theta \in [0, 2\pi)$ . Note that we have abbreviated  $\cos\theta$  and  $\sin\theta$  to  $c$  and  $s$  in Eq. (71), respectively. Let us view the probability distribution  $\mathbb{P}(X_t = x)$  when the initial state is given by  $|\Psi_0\rangle = |0\rangle \otimes (1/\sqrt{2} |0\rangle + i/\sqrt{2} |1\rangle)$ . The operator in Eq. (71) can give rise to probability distributions which have four sharp peaks, as shown in **Figure 9**. These four peaks can also be observed at relatively small time in **Figure 10**. Seeing **Figure 11**, we guess some values of the parameter  $\theta$  when the number of sharp peaks is three. They are  $\pi/3, 2\pi/3, 4\pi/3$ , and  $5\pi/3$ , and these values can be exactly estimated by a limit theorem which will be introduced later.

We find a long-time limit theorem in the paper [8] and it asserts the convergence of a random variable rescaled by time  $t$ .

**Theorem 4** Assume that  $\theta \neq 0, \pi/2, \pi, 3\pi/2$ . For a real number  $x$ , we have

$$\begin{aligned}
 \lim_{t \rightarrow \infty} \mathbb{P}\left(\frac{X_t}{t} \leq x\right) &= \int_{-\infty}^x \left[ \{1 - \nu(\alpha, \beta; y)\} f(y) I_{\left(\frac{1-4c^2}{3}, \frac{\sqrt{1+8c^2}}{3}\right)}(y) \right. \\
 &\quad \left. + \{1 + \nu(\alpha, \beta; -y)\} f(-y) I_{\left(\frac{\sqrt{1+8c^2}}{3}, \frac{1-4c^2}{3}\right)}(y) \right] dy,
 \end{aligned}
 \tag{72}$$

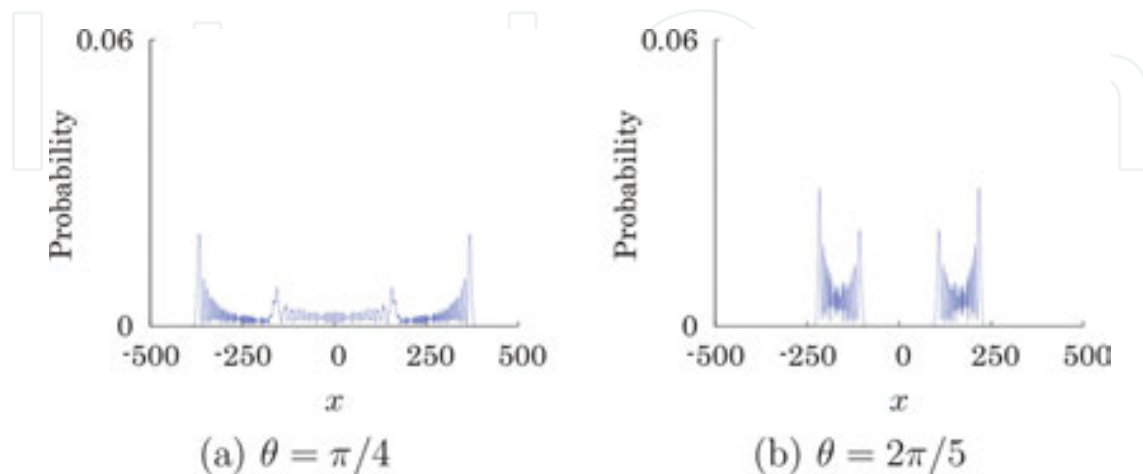


**Figure 9.** Probability distribution at time 500 ( $\alpha = 1/\sqrt{2}, \beta = i/\sqrt{2}$ ).

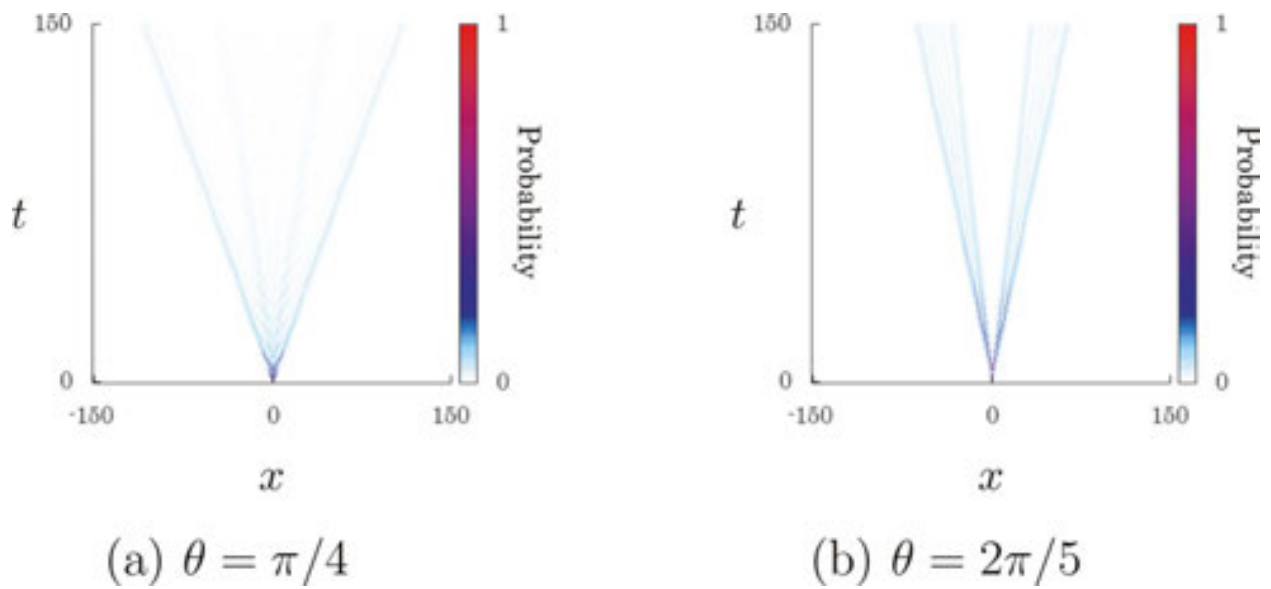


Figure 10. Time evolution of the probability distribution ( $\alpha=1/\sqrt{2}$ ,  $\beta=i/\sqrt{2}$ ).

where

$$f(x) = \frac{|s| \left( |s|x + \sqrt{D(x)} \right)^2}{\pi(1-x^2)\sqrt{W_+(x)}\sqrt{W_-(x)}\sqrt{D(x)}}, \tag{73}$$

$$\begin{aligned} \nu(\alpha, \beta; x) = & \frac{1}{c(1+8c^2)} \{9c^3(|\alpha|^2 - |\beta|^2) + 3s(1+6c^2)\Re(\alpha\bar{\beta})\} x \\ & + \frac{s}{c|s|(1+8c^2)} \{cs(|\alpha|^2 - |\beta|^2) - (1+2c^2)\Re(\alpha\bar{\beta})\} \sqrt{D(x)}, \end{aligned} \tag{74}$$

$$D(x) = 1 + 8c^2 - 9c^2x^2, \tag{75}$$

$$W_+(x) = -(1-4c^2) + 3(1-2c^2)x^2 + 2|s|x\sqrt{D(x)}, \tag{76}$$

$$W_-(x) = 1 + 8c^2 - 3(1+2c^2)x^2 - 2|s|x\sqrt{D(x)}, \tag{77}$$

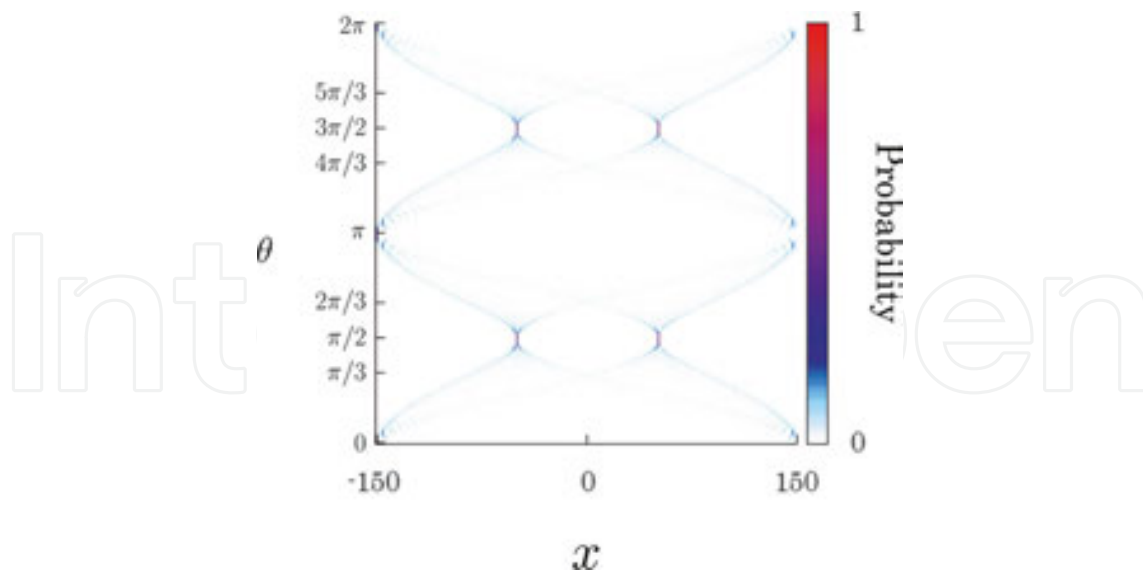


**Figure 11.** This picture shows how the probability distribution at time 150 depends on the value of the parameter  $\theta$ . ( $\alpha=1/\sqrt{2}$ ,  $\beta=i/\sqrt{2}$ ).

and  $\Re(z)$  denotes the real part of the complex number  $z$ .

This limit theorem can be derived by Fourier analysis as well. For the Fourier transform  $|\hat{\Psi}_t(k)\rangle = \sum_{x \in \mathbb{Z}} e^{-ikx} |\psi_t(x)\rangle$  ( $k \in [-\pi, \pi)$ ), Eq. (68) produces a time evolution of the Fourier transform,

$$\begin{aligned} |\hat{\psi}_{3t}(k)\rangle &= \{R(k)(R(k)U)^2\}^t |\hat{\Psi}_0(k)\rangle, \\ |\hat{\psi}_{3t+1}(k)\rangle &= R(k)U \{R(k)(R(k)U)^2\}^t |\hat{\Psi}_0(k)\rangle, \\ |\hat{\psi}_{3t+2}(k)\rangle &= (R(k)U)^2 \{R(k)(R(k)U)^2\}^t |\hat{\Psi}_0(k)\rangle. \end{aligned} \tag{78}$$

Given an orthogonal normalized basis such as Eq. (29), the matrix

$$R(k)(R(k)U)^2 = \begin{bmatrix} c^2 e^{3ik} + s^2 e^{ik} & cse^{3ik} - cse^{ik} \\ -cse^{-3ik} + cse^{-ik} & c^2 e^{-3ik} + s^2 e^{-ik} \end{bmatrix} \tag{79}$$

has two eigenvalues

$$\lambda_j(k) = c^2 \cos 3k + s^2 \cos k - (-1)^j i \sqrt{1 - (c^2 \cos 3k + s^2 \cos k)^2} \quad (j = 1, 2). \tag{80}$$

A possible expression of the normalized eigenvector associated to the eigenvalue  $\lambda_j(k)$  is

$$|v_j(k)\rangle = \frac{1}{\sqrt{N_j(k)}} \left[ \frac{-2cse^{2ik} \sin k}{c^2 \sin 3k + s^2 \sin k + (-1)^j \sqrt{1 - (c^2 \cos 3k + s^2 \cos k)^2}} \right], \quad (81)$$

where  $N_j(k)$  is the normalization factor

$$N_j(k) = 2 \left\{ 1 - (c^2 \cos 3k + s^2 \cos k)^2 + (-1)^j (c^2 \sin 3k + s^2 \sin k) \sqrt{1 - (c^2 \cos 3k + s^2 \cos k)^2} \right\}. \quad (82)$$

With a decomposition  $|\hat{\Psi}_{3t}(k)\rangle = \sum_{j=1}^2 \lambda_j^t(k) \langle v_j(k) | \hat{\Psi}_0(k) \rangle |v_j(k)\rangle$ , we get representations in the eigenspace,

$$|\hat{\psi}_{3t}(k)\rangle = \sum_{j=1}^2 \lambda_j^t(k) \langle v_j(k) | \hat{\psi}_0(k) \rangle |v_j(k)\rangle, \quad (83)$$

$$|\hat{\psi}_{3t+1}(k)\rangle = R(k)U \sum_{j=1}^2 \lambda_j^t(k) \langle v_j(k) | \hat{\psi}_0(k) \rangle |v_j(k)\rangle, \quad (84)$$

$$|\hat{\psi}_{3t+2}(k)\rangle = (R(k)U)^2 \sum_{j=1}^2 \lambda_j^t(k) \langle v_j(k) | \hat{\psi}_0(k) \rangle |v_j(k)\rangle, \quad (85)$$

and compute their derivatives

$$\frac{d^r}{dk^r} |\hat{\psi}_{3t}(k)\rangle = (t)_r \sum_{j=1}^2 \lambda_j^{t-r}(k) \lambda_j^r(k) \langle v_j(k) | \hat{\psi}_0(k) \rangle |v_j(k)\rangle + O(t^{r-1}), \quad (86)$$

$$\begin{aligned} \frac{d^r}{dk^r} |\hat{\psi}_{3t+1}(k)\rangle &= (t)_r R(k)U \sum_{j=1}^2 \lambda_j^{t-r}(k) \lambda_j^r(k) \langle v_j(k) | \hat{\psi}_0(k) \rangle |v_j(k)\rangle \\ &+ O(t^{r-1}), \end{aligned} \quad (87)$$

$$\begin{aligned} \frac{d^r}{dk^r} |\hat{\psi}_{3t+2}(k)\rangle &= (t)_r (R(k)U)^2 \sum_{j=1}^2 \lambda_j^{t-r}(k) \lambda_j^r(k) \langle v_j(k) | \hat{\psi}_0(k) \rangle |v_j(k)\rangle \\ &+ O(t^{r-1}). \end{aligned} \quad (88)$$

The moments  $E(X_{3t}^r)$ ,  $E(X_{3t+1}^r)$ , and  $E(X_{3t+2}^r)$  turn out to be of the form

$$(t)_r \cdot \sum_{j=1}^2 \frac{1}{2\pi} \int_{-\pi}^{\pi} \left( \frac{i\lambda_j'(k)}{\lambda_j(k)} \right)^r |\langle v_j(k) | \hat{\psi}_0(k) \rangle|^2 dk + O(t^{r-1}), \quad (89)$$

and we see

$$\begin{aligned} \lim_{t \rightarrow \infty} \mathbb{E} \left[ \left( \frac{X_{3t}}{3t} \right)^r \right] &= \lim_{t \rightarrow \infty} \mathbb{E} \left[ \left( \frac{X_{3t+1}}{3t+1} \right)^r \right] = \lim_{t \rightarrow \infty} \mathbb{E} \left[ \left( \frac{X_{3t+2}}{3t+2} \right)^r \right] \\ &= \sum_{j=1}^2 \frac{1}{2\pi} \int_{-\pi}^{\pi} \left( \frac{i\lambda_j'(k)}{3\lambda_j(k)} \right)^r |\langle v_j(k) | \hat{\psi}_0(k) \rangle|^2 dk, \end{aligned} \quad (90)$$

which is put together as

$$\lim_{t \rightarrow \infty} \mathbb{E} \left[ \left( \frac{X_t}{t} \right)^r \right] = \sum_{j=1}^2 \frac{1}{2\pi} \int_{-\pi}^{\pi} \left( \frac{i\lambda_j'(k)}{3\lambda_j(k)} \right)^r |\langle v_j(k) | \hat{\psi}_0(k) \rangle|^2 dk, \quad (91)$$

where

$$\frac{i\lambda_j'(k)}{3\lambda_j(k)} = (-1)^j \frac{3c^2 \sin 3k + s^2 \sin k}{3\sqrt{1 - (c^2 \cos 3k + s^2 \cos k)^2}}. \quad (92)$$

Setting  $i\lambda_j'(k)/3\lambda_j(k) = x$  ( $j=1, 2$ ) in Eq. (91) leads us to an integral expression of the limit,

$$\begin{aligned} \lim_{t \rightarrow \infty} \mathbb{E} \left[ \left( \frac{X_t}{t} \right)^r \right] &= \int_{-\infty}^{\infty} x^r \left[ \{1 - \nu(\alpha, \beta; x)\} f(x) I_{\left( \frac{1-4c^2}{3}, \frac{\sqrt{1+8c^2}}{3} \right)}(x) \right. \\ &\quad \left. + \{1 + \nu(\alpha, \beta; -x)\} f(-x) I_{\left( -\frac{\sqrt{1+8c^2}}{3}, -\frac{1-4c^2}{3} \right)}(x) \right] dx, \end{aligned} \quad (93)$$

which guarantees Theorem 4. **Figure 12** shows the limit density function  $(d/dx)\mathbb{P}(X_t/t \leq x)$  when  $\alpha=1/\sqrt{2}$ ,  $\beta=i/\sqrt{2}$ , and we view the features of **Figure 9** in the limit density function. The density function contains singular points at  $\pm(1-4c^2)/3$ ,  $\pm\sqrt{1+8c^2}/3$ . When  $\theta = \pi/4$ , they are found at

$\pm 1/3 (= \pm 0.333 \dots)$ ,  $\pm \sqrt{5}/3 (= \pm 0.745 \dots)$  in **Figure 12-(a)**, and when  $\theta = 2\pi/5$ , at  $\pm(\sqrt{5}-1)/6 (= \pm 0.206 \dots)$ ,  $\pm\sqrt{4-\sqrt{5}}/3 (= \pm 0.442 \dots)$  in **Figure 12-(b)**.

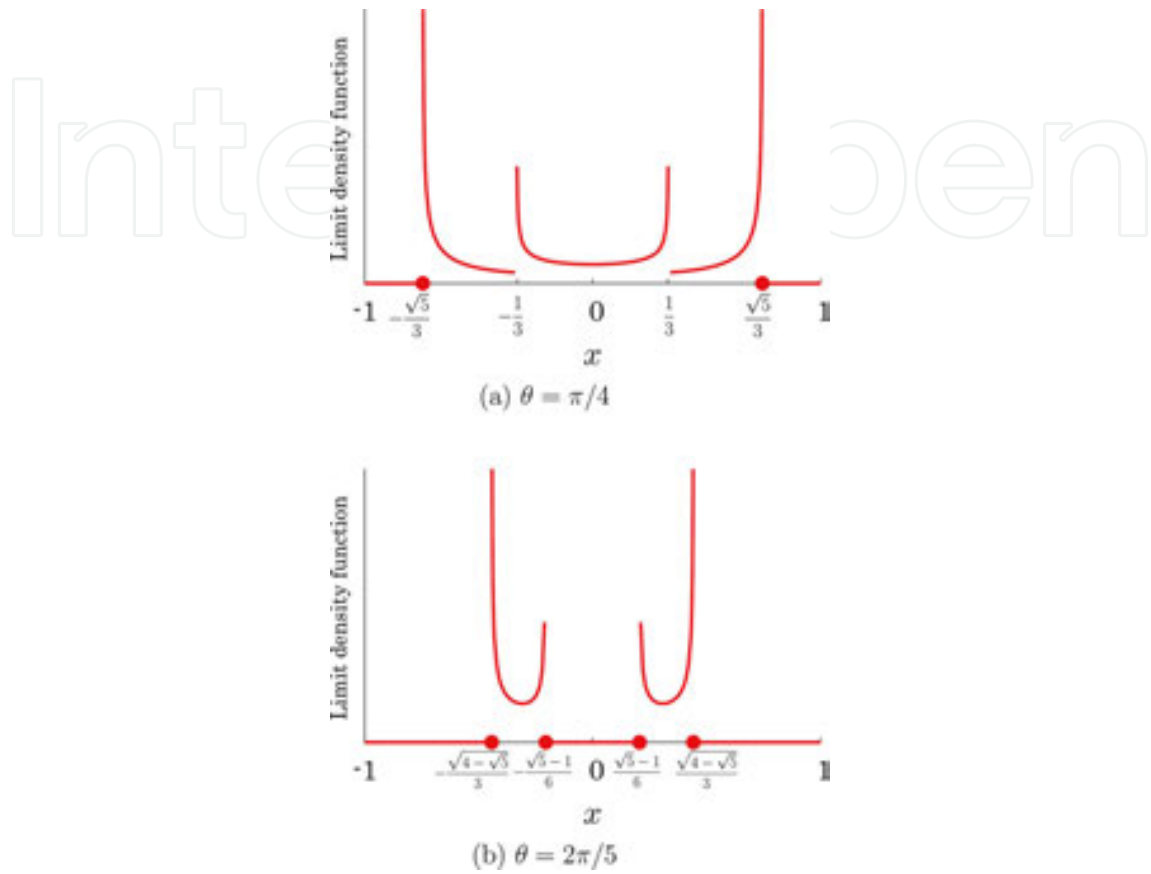


**Figure 12.** Limit density function ( $\alpha = 1/\sqrt{2}$ ,  $\beta = i/\sqrt{2}$ ).

### Acknowledgements

The author is supported by JSPS Grant-in-Aid for Young Scientists (B) (No. 16K17648).

### Author details

Takuya Machida

Address all correspondence to: tz14040@meiji.ac.jp

College of Industrial Technology, Nihon University, Narashino, Chiba, Japan

## References

- [1] S. P. Gudder (1988), *Quantum probability*, Academic Press. Probability and Mathematical Statistics.
- [2] Y. Aharonov, L. Davidovich and N. Zagury (1993), *Quantum random walks*, Phys. Rev. A, 48(2), pp. 1687–1690.
- [3] D. A. Meyer (1996), *From quantum cellular automata to quantum lattice gases*, Journal of Statistical Physics, 85(5–6), pp. 551–574.
- [4] S. E. Venegas-Andraca (2012), *Quantum walks: a comprehensive review*, Quantum Information Processing, 11(5), pp. 1015–1106.
- [5] N. Konno (2002), *Quantum random walks in one dimension*, Quantum Information Processing, 1(5), pp. 345–354.
- [6] G. Grimmett, S. Janson and P.F. Scudo (2004), *Weak limits for quantum random walks*, Phys. Rev. E, 69(2), p. 026119.
- [7] T. Machida and N. Konno (2010), *Limit theorem for a time-dependent coined quantum walk on the line*, F. Peper et al. (Eds.): IWNC 2009, Proceedings in Information and Communications Technology, 2, pp. 226–235.
- [8] F. A. Grünbaum and T. Machida (2015), *A limit theorem for a 3-period time-dependent quantum walk*, Quantum Information and Computation, 15(1& 2), pp. 50–60.

IntechOpen

